LAWRENCE
LIVERMORE
NATIONAL
LABORATORY

LLNL-TR-667466

Steady State Sputtering Yields and Surface Compositions of Depleted Uranium and Uranium Carbide bombarded by 30 keV Gallium or 16 keV Cesium Ions.

W. J. Siekhaus, N. E. Teslich, P. K. Weber

February 18, 2015

Disclaimer

This work performed under the auspices of the U.S. Department of Energy by Lawrence Livermore National Laboratory under Contract DE-AC52-07NA27344.

Steady state sputtering yields and surface compositions of depleted uranium and uranium carbide bombarded by 30keV gallium or 16keV cesium ions.

Wigbert J. Siekhaus , Nick E. Teslich Jr., Peter K. Weber

Lawrence Livermore National Laboratory, Livermore, CA 94551-9234, USA

Depleted uranium that included carbide inclusions was sputtered with 30keV gallium ions or 16kev cesium ions to depths much greater than the ions' range, i.e. using steady state sputtering. The recession of both the uranium's and uranium carbide's surfaces and the ion corresponding fluences were used to determine the steady state target sputtering yields of both uranium and uranium carbide, i.e. 6.3 atoms of uranium and 2.4 units of uranium carbide eroded per gallium ion, and 9.9 uranium atoms and 3.65 units of uranium carbide eroded by cesium ions. The steady state surface composition resulting from the simultaneous gallium or cesium implantation and sputter-erosion of uranium and uranium carbide were calculated to be $U_{86}Ga_{14}$, $(UC)_{70}Ga_{30}$ and $U_{81}Cs_9$, $(UC)_{79}Cs_{21}$, respectively.

I. INTRODUCTION

Gallium ions are routinely used in focused ion beam etching (FIB) in secondary electron microscopy (SEM) to investigate the sub-surface structure and composition in situ or to produce "lift-outs" for transmission electron microscopy (TEM). Cesium ions are employed in secondary ion mass spectroscopy (SIMS) (Benninghoven[1]) to remove surface contamination, to determine the depth distribution of elements, and to increase the emission of negative ions for mass analysis by changing the work function of the surface (Krohn[2]). In both applications knowledge of the sputtering yield Y, defined here as entities (atoms or molecules) of substrate sputtered per incident ion, is needed to predict surface recession rates. There are equations to calculate the initial sputtering yields of pure monatomic solids (Yamamura[3] and Behrisch[4]) and computer simulations for monatomic solids and compounds (Eckstein[5]) of initial sputtering yields as well as yields during steady state sputtering, i.e. when the depth of erosion exceeds the depth of penetration of the sputtering ions. These equations and simulations fit many available experimental data well, but experimental data for gallium or cesium initial sputtering of pure uranium or uranium carbide are not found in the literature, and neither are sputtering yields under steady state conditions. Here we determine the steady state yields of gallium and cesium sputtering uranium and uranium carbide, compare them with modeled initial sputtering yields for pure materials, and calculate the steady state surface concentrations for uranium and uranium carbide inclusions in uranium, materials of importance in the nuclear industry.

II. EXPERIMENTAL

The depleted uranium (D238) sample was cast, cut and polished by Los Alamos National Laboratory[6] and has a carbon weight content of approximately 100 ppm weight and a hydrogen weight content of approximately 1 ppm weight. The uranium carbide inclusions appear white in the optical micrograph shown in figure 1. Recent work[7] has shown that the carbide inclusions also include nitrogen. Areas including a carbide were selected and bombarded by either 2.8 nA of 30 keV Ga ions in a FIB-FESEM[8] or 16 keV Cs ions (of either 370 or 1000 pA) in a "NanoSIMS"[9]. The Ga-sputtering-induced recession of the surface was measured in situ in the FIB-FESEM after tilting the surface by 50 degrees and confirmed ex situ using a stylus profilometer, while the Cs-sputtering recession was measured only ex situ using a profilometer.

III. Results

A. Steady state sputtering with 30keV gallium ions

Figure 2 is an SEM image of the sputtered area (20μm x 20 μm) after a sputtering time of 5 minutes. It includes part of a carbide particle. Sputtering was interrupted in one-minute intervals to measure the depth of recession of the uranium and of the uranium carbide, respectively. The results of the recession measurements are shown in figure 5, from which *average* recession rates of 0.34153 μm/min and .1821 μm/min are derived for uranium and uranium carbide, respectively. The recession rates can be converted to steady state sputtering yields of $Y^{U}_{30\text{keV Ga}\rightarrow\text{U, measured}} = 6.3$ atoms per gallium ion, and of $Y^{UC}_{30\text{keV Ga}\rightarrow\text{UC, measured}} = 2.3$ uranium carbide units per gallium ion, respectively, using the gallium current of 2.8 nA and the area of 400 μm^2.

B. *Steady state sputtering with 16keV cesium ions*

Ten areas ranging in size from 40x40µm to 100x100µm were sputtered with cesium ions of 16 keV energy in the SIMS instrument using currents from 370 pA to 1000 pA and durations from 1 hour to 13.5 hour. Three of these areas contained carbide particles. Figure 3 is an SEM image of such an area. The depths of the sputtered craters were measured by stylus profilometry. The results are summarized in table 1, and show specific volume removal rates of 1.28 (μm^2 nm/pA s) and .66 (μm^2 nm/pA s) for uranium and uranium carbide, respectively, equivalent to sputtering yields of $Y^{U}_{16keV\ Cs \rightarrow U,\ measured}$= 9.91 atoms uranium per cesium ion, and of $Y^{UC}_{16keVCs \rightarrow UC,\ measured}$= 3.7 uranium carbide units per cesium ion.

IV. Discussion

A. *Sputtering yields and surface composition*

The initial yields of 30 keV gallium and 16 keV cesium sputtering pure uranium calculated using Yamamura's equations are $Y^{U}_{30keV\ Ga \rightarrow U,\ Yamamura} = 7.74$ and $Y^{U}_{16keV\ Cs \rightarrow U,\ Yamamura} = 9.14$, higher by about 1.5 for gallium and lower by about 0.5 for cesium than our measured values. Yamamura's equations apply to the initial sputtering of pure elements only, and hence cannot be applied to uranium carbide or the compounds created during steady state sputtering due to ion implantation. Our measured sputtering yields are not the yields that the first ion impinging on a pristine uranium or uranium carbide surface would produce, but rather are the steady state sputtering yields from an uranium+(gallium or cesium) compound and uranium carbide +(gallium or cesium) compound, respectively, that is created by the concomitant process of ion implantation during sputtering. The surface composition of compounds will be discussed below. Steady state sputtering (also called stoichiometric sputtering since the stoichiometry of the sputtered flux is the same as that of the target) is reached when a layer larger than the range of implanted ions is removed by sputtering. TRIM[10] code calculations produce an implantation depth distribution function with an average depth of penetration into uranium of 50 nm and of 109 nm for 16keV cesium and 30 keV gallium ions, respectively[11]. That mean depth is much smaller than the depth of the craters used for measuring the sputtering yields. At steady state one atom of the implant species i is sputtered for each ion i bombarding the target element j. Hence at steady state the sputtering yield $Y^{\boldsymbol{i}}_{\boldsymbol{i}\to\boldsymbol{j}}=1$ for all energies, while $Y^{\boldsymbol{j}}_{\boldsymbol{i}\to\boldsymbol{j}}$ is the measured sputtering yield of target $\boldsymbol{j}$ deduced from the surface recession of j. Experiments have shown that sputtered atoms originate almost exclusively from the first atomic layers of the substrate[12]. Eckstein[13] has shown that during steady state sputtering by a noble gas ion $\boldsymbol{k}$ the surface concentrations of elements $\boldsymbol{l}$ and $\boldsymbol{m}$ of a compound consisting of elements $\boldsymbol{l}$ and $\boldsymbol{m}$ depend on the energy of $\boldsymbol{k}$, and at energies below 10keV deviate substantially from the bulk stoichiometric composition due to preferential sputtering of either $\boldsymbol{l}$ or $\boldsymbol{m}$. However, with increasing ion energy the surface composition approaches the bulk composition, such that e.g. for 15 keV argon or xenon sputtering of tungsten carbide ($W_{50}C_{50}$) the surface composition is ($W_{55}C_{45}$) during steady state sputtering. Concerning the compound formed due to ion implantation, Gnaser[14] has similarly shown that at energies below 5 keV the surface composition during the *initial* stages of cesium sputtering of pure semiconductors is determined by preferential sputtering. It is reasonable to assume that the compound formed during *high energy steady state* gallium and cesium sputtering of uranium and uranium carbide behaves similarly to high energy sputtering of compounds described by Eckstein, i.e. that the stoichiometry of the sputtered material flux (1 unit of cesium or gallium and Y units of substrate, where Y is the measured sputtering yield) approaches closely the stoichiometry of the surface. Then the surface concentration of the sputtering ion ***i*** on the surface of ***j*** is given by

$$CS^{i}_{i->j} = \frac{1}{1+Y^{j}_{i->j}} \qquad (1)$$

Equation (1) has been frequently used in earlier publications[15-20], making use of the measured values $Y^{j}_{i\rightarrow j}$ or even values calculated using the equations that are in reality only applicable to initial sputtering of pure materials. The surface concentrations derived using equation (1) are listed in table 2.

B. Surface structure of sputtered uranium and uranium carbide

After sputtering, the surface structure of uranium carbide differs greatly from that of uranium metal. The metal surface is greatly roughened, particularly visible after deep gallium sputtering shown in figure 2, while the uranium carbide surface shows no roughening at all. Similarly, cesium-sputtered craters of low depth (figure 3) as well as those of greater depth again (figure 4) show the surfaces of carbide inclusions to be smooth and the uranium surface to be rough. Sputtering-induced surface roughening has been observed frequently[20], and often is attributed to the dependence of the sputtering coefficient on crystal orientation, with the consequence that e.g. in polycrystalline copper roughened surface areas, areas with pyramidal spikes and smooth surfaces appear[21] after sputtering with 10 keV krypton at normal incidence and a fluence of 10^{18} atoms/cm^{2}. Figures 3 and 4 suggest that all faces of the carbide inclusions sputter without roughing.

V. SUMMARY AND CONCLUSIONS

We provide measurements of the steady state sputtering yield of gallium and cesium bombarding uranium and uranium carbide targets and calculate the resulting surface concentrations of gallium and cesium on both targets. We note the significant difference in sputtering induced surface roughening between uranium carbide and uranium metal.

ACKNOWLEDGMENTS

The authors thank Ian Hutcheon and Jenny Matzel for discussions and Christina Ramon for technical assistance. Prepared by Lawrence Livermore National Laboratory under Contract DE-AC52-07NA27344.

Figures

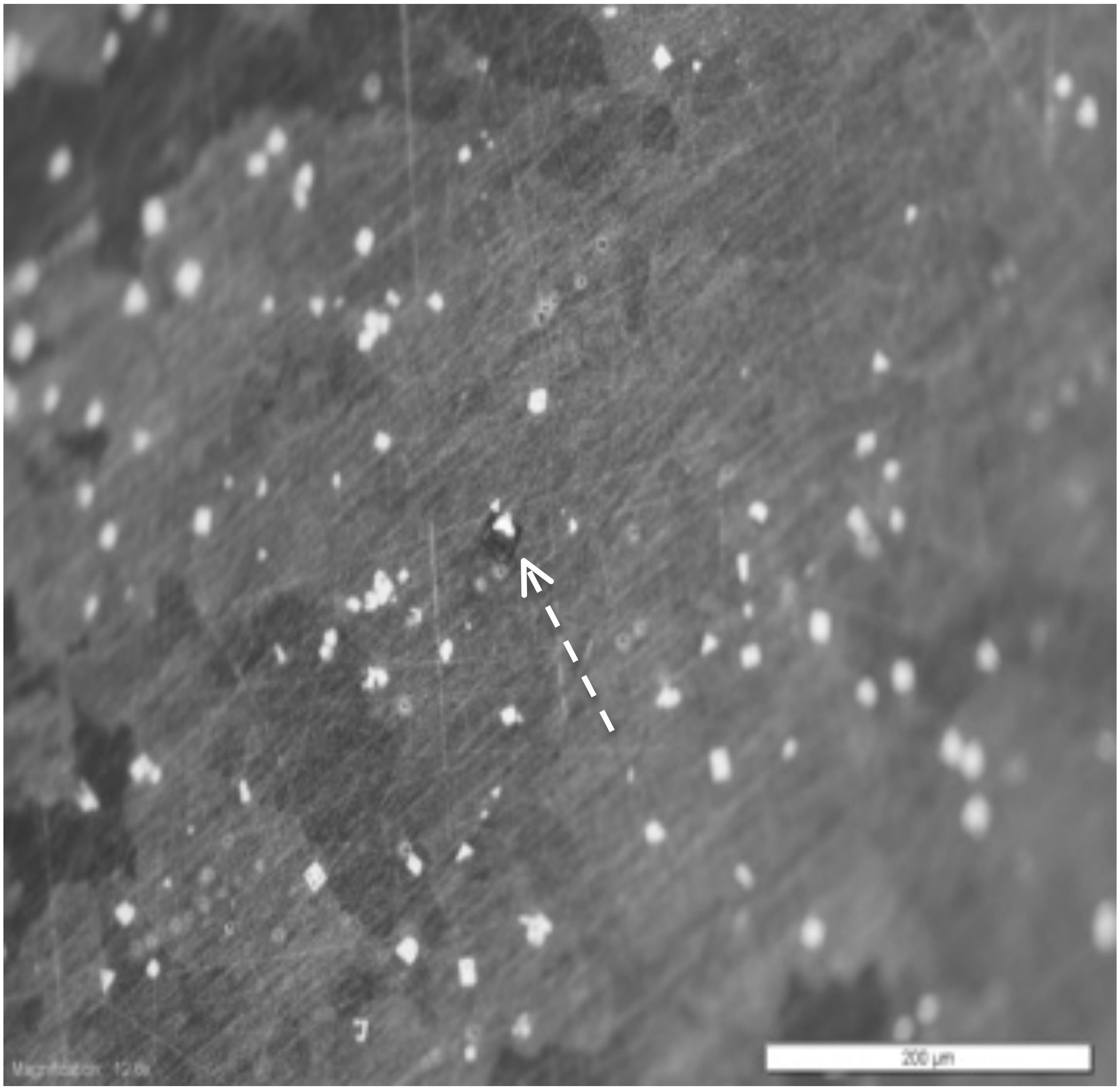

Figure 1.

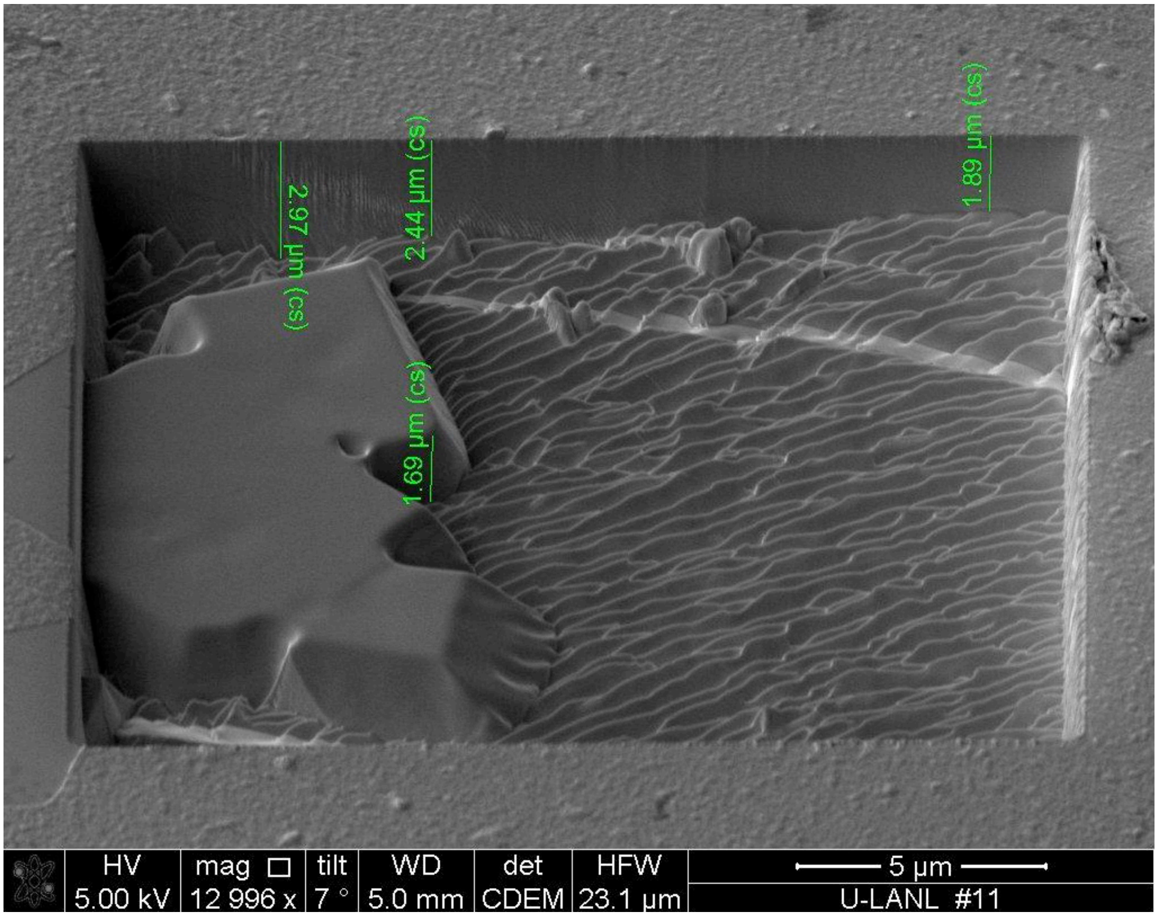
2.97 µm (cs)
2.44 µm (cs)
1.89 µm (cs)
1.69 µm (cs)
HV
5.00 kV
mag ☐
12 996 x
tilt
7 °
WD
5.0 mm
det
CDEM
HFW
23.1 µm
5 µm
U-LANL #11

Figure 2.

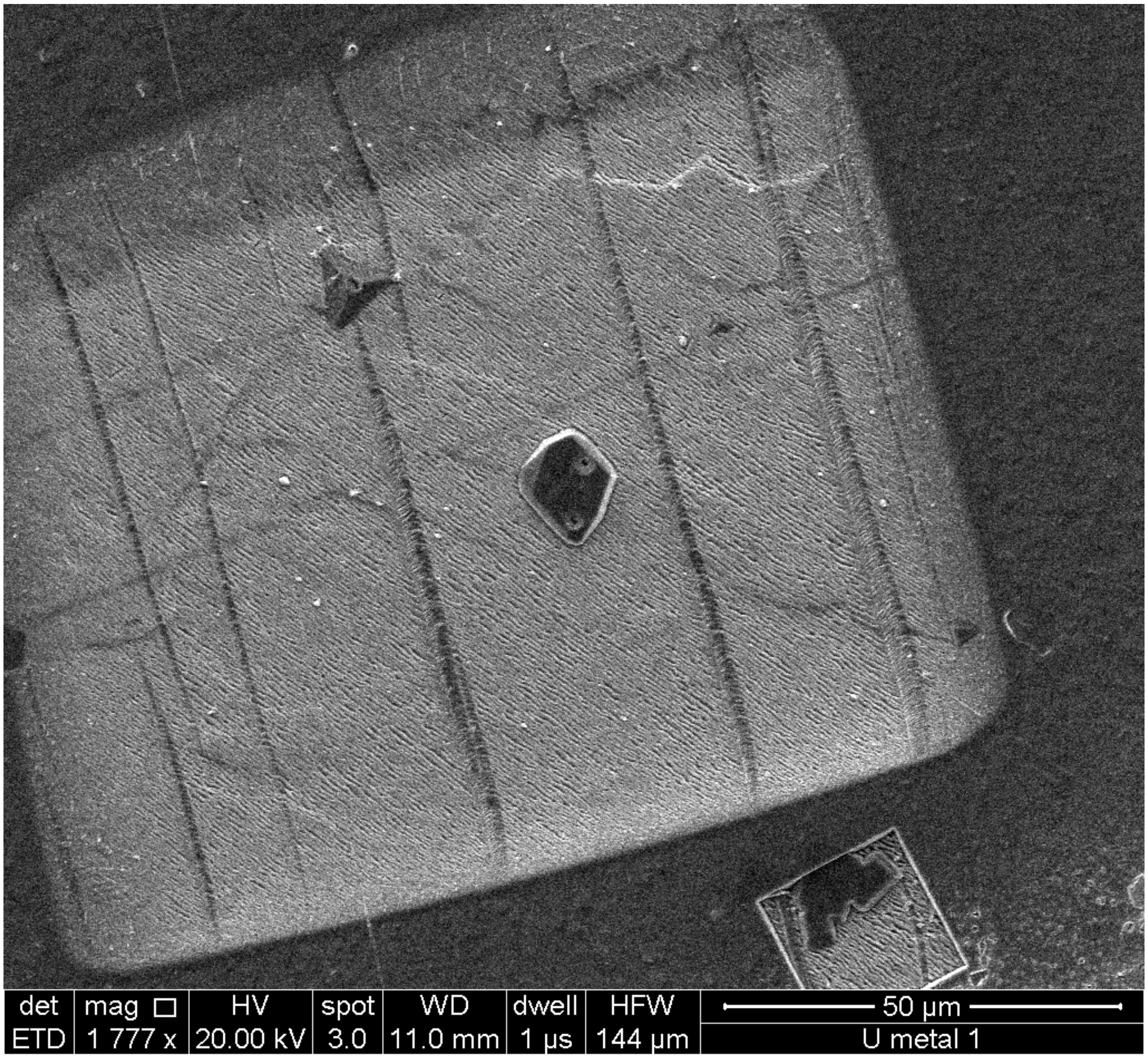
det
mag
HV
spot
WD
dwell
HFW
50 µm
ETD
1 777 x
20.00 kV
3.0
11.0 mm
1 µs
144 µm
U metal 1

Figure 3.

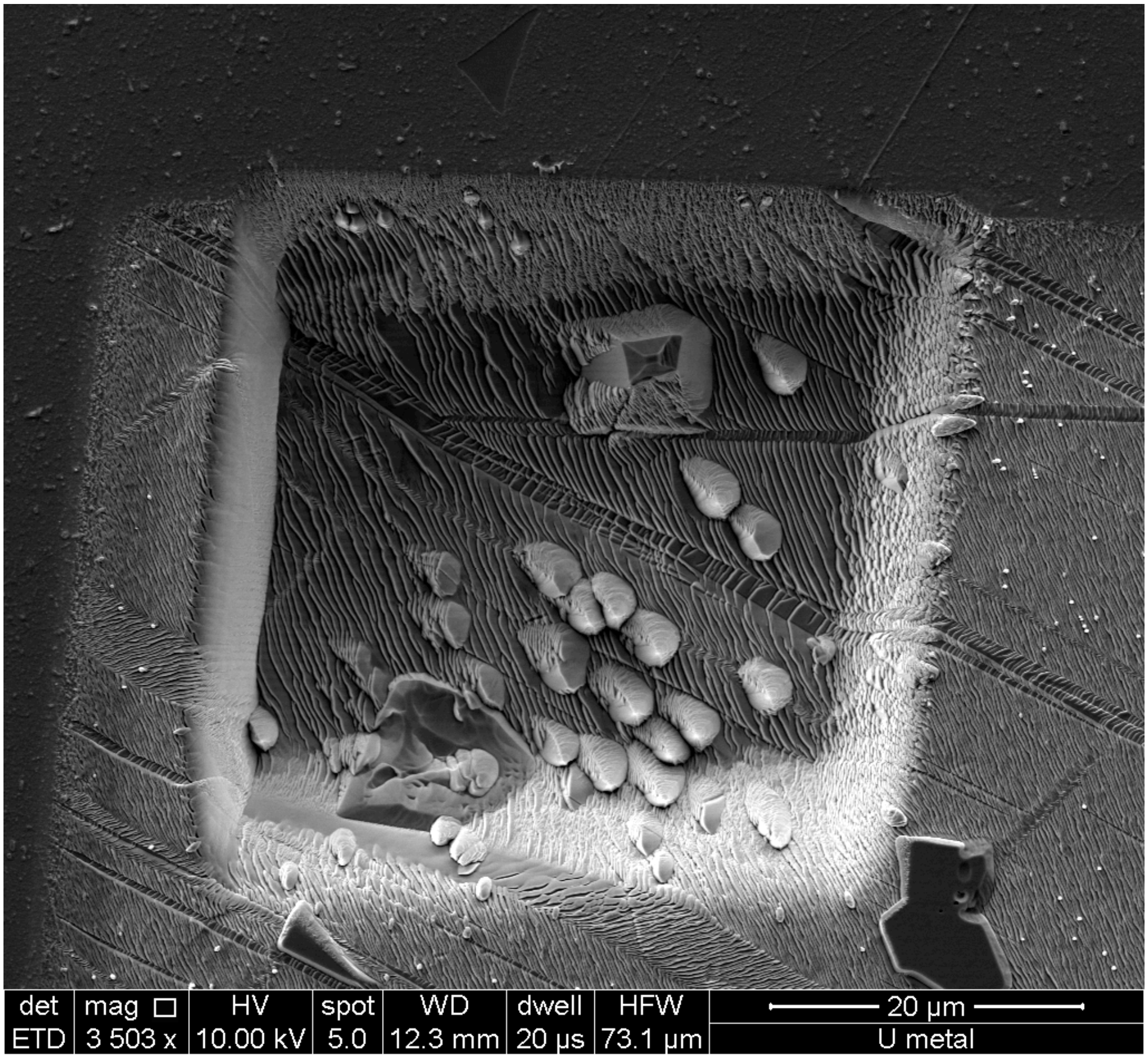
det
mag □
HV
spot
WD
dwell
HFW
20 µm
ETD
3 503 x
10.00 kV
5.0
12.3 mm
20 µs
73.1 µm
U metal

Figure 4

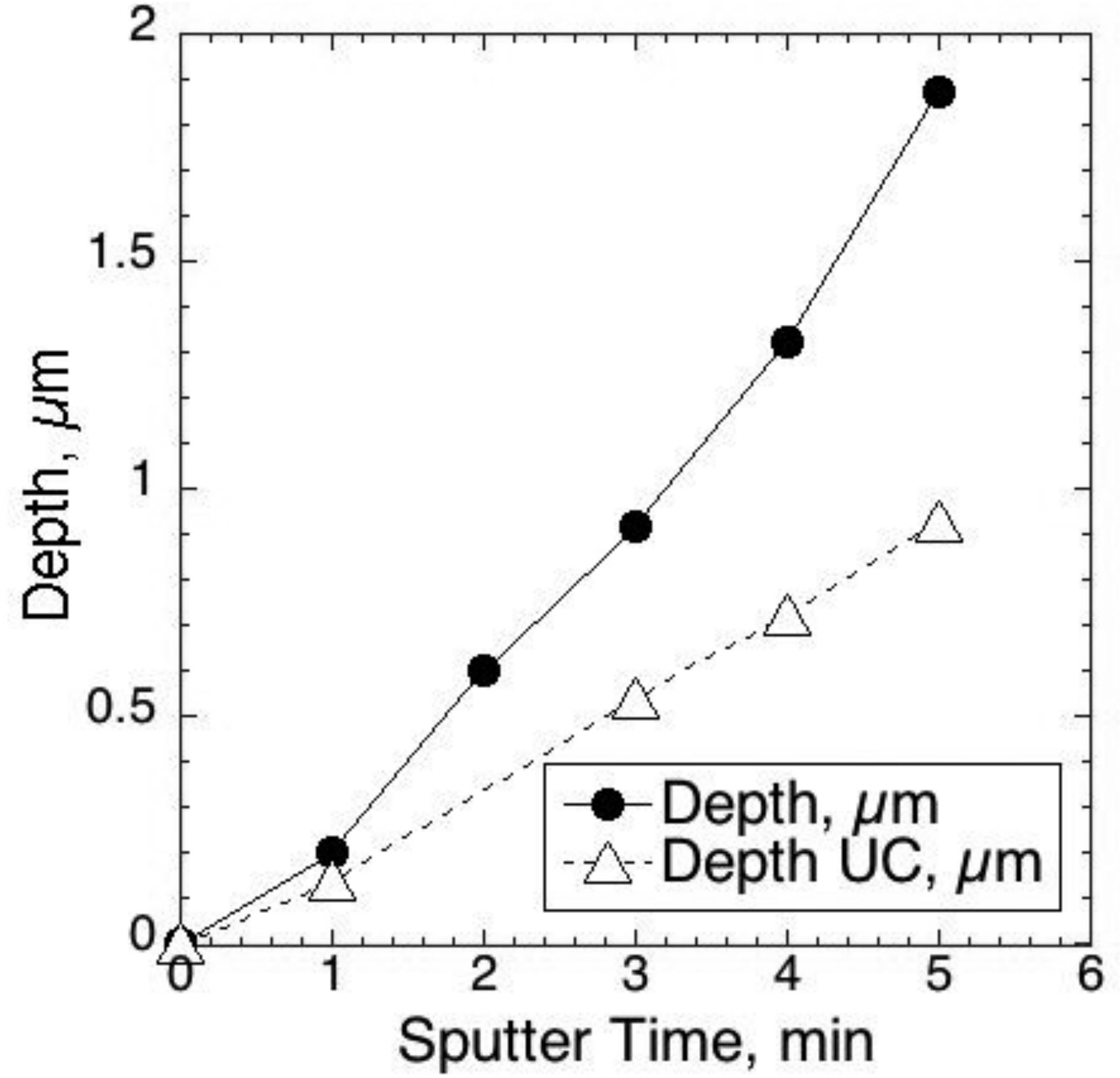
2
1.5
1
0.5
0
Depth, μm
0
1
2
3
4
5
6
Sputter Time, min
Depth, μm
Depth UC, μm

Figure 5

Tables

Table 1

Area #	Sputter current (pA)	Duration (hr)	Nominal raster size (µm)	Measured raster area (µm^2)	Measured depth (nm)	Sputter rate (µm^{2}nm/pAs)	Material	Depth (nm)	Sputter rate (µm^{2}nm/pAs)	Material
A5	370	11	100	9,540	1,200	0.87	U			
A6	1000	6	100	11,300	2,600	1.36	U	877	.60	UC$_x$
A7	1000	12.5	110	12,600	4,800	1.34	U			
A8	1000	18	110	11,500	7,500	1.33	U			
A9	1000	5	100	11,136	2,750	1.53	U	1,273	0.71	UC$_x$
A10	370	805	100	9,975	1,500	1.32	U			
A10	370	13.5	40	1,600	9,071	0.81	U			
A11	370	10.5	60	3,528	5,779	1.45	U			
A12	370	4.5	60	3,420	2,485	1.50	U			
A13	1000	1	60	3,933	1,168	1.28	U	629	0.69	UC$_x$
-------	-------	-----	-------	-------	---------	--------	----	-------	-------	------
					Median	1.34	U		.69	UC$_x$
					Average	1.28	U		.66	UC$_x$
					SE	.08	U		0.03	UC$_x$
					N	10	U		3	UC$_x$

Table 2

Sputter Ion @ Energy	Target	Sputtering Yield	Calculated Surface Composition
Gallium @ 30 keV	Uranium	$Y^{U}_{\text{30keV Ga}\rightarrow\text{U, measured}}= 6.3$ $Y^{Ga}_{\text{30keV Ga}\searrow\text{UC}} = 1$	$U_{86}Ga_{14}$
Gallium @ 30 keV	Uranium Carbide	$Y^{UC}_{\text{16keV Cs}\rightarrow\text{UC}}= 2.3$ $Y^{Cs}_{\text{16keV Cs}\searrow\text{UC}}= 1$	$(UC)_{70}Ga_{30}$
Cesium @ 16 keV	Uranium	$Y^{U}_{\text{16keV Cs}\rightarrow\text{U}}= 9.91$ $Y^{Cs}_{\text{16keV Cs}\searrow\text{U}}= 1$	$U_{81}Cs_{9}$
Cesium @ 16 keV	Uranium Carbide	$Y^{UC}_{\text{16keVCs}\rightarrow\text{UC}}=3.7$ $Y^{Cs}_{\text{16keV Cs}\searrow\text{UC}}= 1$	$(UC)_{79}Cs_{21}$

Figure Captions

Figure 1. Optical micrograph of the polished uranium surface, showing the carbon inclusions in white. The white dashed arrow points to he black square in the center including a white triangular-shaped carbide inclusion where the Ga ion sputtering had been performed.

Figure 2. SEM image of the Ga-ion sputtered area, showing a smooth carbide surface and a roughened uranium surface.

Figure 3. SEM image of lightly Cs-ion sputtered area 9, showing carbide surfaces smoother than the uranium metal surface.

Figure 4. SEM image of heavily Cs-ion sputtered area 11 within lightly sputtered area 10, showing carbide surfaces smoother than the uranium metal surface.

Figure 5. Depth of the sputtered uranium and of the uranium carbide surface, respectively, as a function of sputtering time.

REFERENCES

[1] R. A. Benninghoven, F. G. Ruedenauer, and H. W. Werner, *Secondary Ion Mass Spectrometry* (Wiley, New York, 1987)

[2] V. E. Krohn, J Appl Phys **33** (1962)

[3] Y. Yamamura, and H. Tawara, Atomic Data and Nuclear Data Tables **62** (1996).

[4] R. Behrisch, and W. Eckstein, *Sputtering by Particle Bombardment. Experiments and Computer Calculations from Threshold to MeV Energy* (Springer Verlag, Heidelberg, 2007), Vol. 110, Top Appl Phys.

[5] J. W. Eckstein, and J. P. Biersack, Appl Phys a-Mater **37** (1985).

[6] R. K. Schulze, 2012, Los Alamos National Laboratory).

[7] T. B. Scott *et al.*, Journal of Hazardous Materials **195** (2011).

[8] FEI, North America Nanoport, 5350 NE Dawson Creek Drive, Hillsboro, Oregon 97214 USA).

[9] CAMECA, Société par Actions Simplifiée (SAS), 29 Quai des Grésillons, 92622 Gennevilliers Cedex – France).

[10] J. P. Biersack, and L. G. Haggmark, Nucl Instrum Methods **174** (1980).

[11] S. Kuchejev, 2012, Lawrence Livermore National Laboratory, Personal Communication.

[12] J. W. Burnett *et al.*, J Vac Sci Technol A **6** (1988).

[13] H. Gnaser, Nucl Instrum Meth B **267** (2009).

[14] J. W. Eckstein, and J. P. Biersack, (1985), ibid.

[15] S. J.E. Chelgren, W. Katz, V.R. Deline, C.A. Evans, R.J. Blattner, P. Williams, J. Vac. Sci. Technol. 16 (1979) 324.

[16] P.A.W. van der Heide, C. Lupu, A. Kutana, J.W. Rabalais, Appl. Surf. Sci. 231–232 (2004) 90.

[17] J. Brison, L. Houssiau, Nucl. Instr. and Meth. B 259 (2007) 984.

[18] M. Vicanek, J.J. Jimenéz-Rodríguez, P. Sigmund, Nucl. Instr. and Meth. B 36 (1989) 124.

[19] Y. Kudriavtsev, Nucl. Instr. and Meth. B 160 (2000) 307.

[20] T. Wirtz, H.-N. Migeon, H. Scherrer, Inter. J. Mass Spectrom. 225 (2003) 135.

[20] G. Carter: in R. Behrisch (Ed.): Sputtering by Particle Bombardment II, Top. Appl. Phys. 52 (Springer, Berlin, Heidelberg 1983) p. 213, russ. translation: (MIR, Moscow 1986)
B. M. U. Scherzer: in R. Behrisch (Ed.): Sputtering by Particle Bombardment II, Top. Appl. Phys. 52 (Springer, Berlin, Heidelberg 1983) p. 271, russ. translation: (MIR, Moscow 1986)

[21] W. Hauffe: Ph.D. Theses A and B, *Techn. Univ. Dresden,* (Dresden 1971)